PROCEEDINGS OF THE ROYAL SOCIETY B

Proc. R. Soc. B (2009) **276**, 1277–1284
doi:10.1098/rspb.2008.1659
Published online 6 January 2009

Development of the five primary podia from the coeloms of a sea star larva: homology with the echinoid echinoderms and other deuterostomes

Valerie B. Morris[1,*], Paulina Selvakumaraswamy[2], Renée Whan[3] and Maria Byrne[2]

[1]*School of Biological Sciences A12,* [2]*Department of Anatomy and Histology, and* [3]*Electron Microscope Unit, University of Sydney, New South Wales 2006, Australia*

Confocal laser scanning microscopy of larvae of the asteroid *Parvulastra exigua* was used to investigate the development of the five primary podia from the coeloms in the echinoderm phylum in an approach to the problem of morphological homology in the deuterostome phyla. The development is shown from an early brachiolaria larval stage to a pre-settlement late brachiolaria larval stage. In the early brachiolaria larva, a single enterocoele connected to the archenteron has formed into two lateral coeloms and an anterior coelom. The primary podia form from the coelomic regions on the left side of the brachiolaria larva, while on the right the coelomic regions connect with the exterior through the pore canal and hydropore. The anterior coelom forms the coelom of the brachia. Homology between the primary podia of the asteroid and the echinoid classes of echinoderms is described and extended to coeloms of other deuterostome phyla.

Keywords: abbreviated larval development; three-dimensional imaging; evolution; sea urchin; *Holopneustes purpurescens*; *Asterina gibbosa*

1. INTRODUCTION

The research we report is directed to the problem of the morphological homology of the deuterostome phyla. It is within the scope of the research into deuterostome evolution, which is wide-ranging, spanning the molecular, palaeontological and morphological fields reviewed recently by Swalla & Smith (2008).

Morphological homology among the deuterostomes is obscure, mostly because the body plans are very different. Echinoderms have a radial body plan that contrasts with the bilateral body plans of the two other principal phyla, the hemichordates and chordates. The approach we take to identify the homology is developmental. The intention is to use evidence of the development of the five primary podia, which are core structures of the echinoderm body plan, to explore whether variation in the development of the primary podia between the echinoderm classes assists in identifying homologous structures in the other phyla. The five primary podia are associated with the growth of the five rays or ambulacra characteristic of the echinoderm phylum (David & Mooi 1996). The development of the five primary podia is described here in the asteroid class of echinoderms. It follows an account of the development of the primary podia in the echinoid class of echinoderms (Morris 2007).

The development of the primary podia is described in *Parvulastra exigua*, formerly *Patiriella exigua*. Larval development in *P. exigua* is lecithotrophic with the larvae reaching the brachiolaria stage with no trace of the bipinnaria feeding stage (Byrne 1995). In this abbreviated development, the formation of the primary podia can be followed more easily than in planktotrophic larvae, because the adult rudiment develops within a few days of fertilization and the structures are larger than in the planktotrophs.

The development of the primary podia and coeloms in *P. exigua* has features in common with *Asterina gibbosa* (MacBride 1896), which, like *P. exigua*, lacks a bipinnaria feeding stage, and with *Asterias rubens* (Gemmill 1914), a species from a different order of the Asteroidea with bipinnaria and brachiolaria larval stages. Although larval development is diverse in asteroids, many features of internal development are retained in the larval types (McEdward & Janies 1993). The early accounts of asteroid development were based on histological serial sections (MacBride 1896; Gemmill 1914). Here, we apply the technique of confocal laser scanning microscopy to preparations of whole larvae of *P. exigua* and use imaging software to construct uninterrupted views into the internal morphology of the larva, showing the coeloms and morphogenesis of the primary podia.

Past schemes that have attempted to derive deuterostome homology through bilaterally paired coelomic structures of the larva (Ubaghs 1967; Peterson *et al.* 2000) have not focused on the primary podia from which the adult phylotypic water vascular system is derived. Here, in contrast, we put the coelomic origins of the primary podia at the start of a search for deuterostome homology. By comparing the coelomic origins of the primary podia in *P. exigua* with those in an echinoid, we identified a conserved relationship between the podia and the inner archenteron, leading us to suggest that sources of deuterostome homology are better looked for in coelomic–archenteron relationships that might be conserved among the deuterostome phyla.

* Author for correspondence (valm@mail.usyd.edu.au).

Received 13 November 2008
Accepted 4 December 2008

2. MATERIAL AND METHODS

Parvulastra exigua were collected from the intertidal zone in New South Wales, Australia, and were spawned and fertilized in the laboratory (Byrne 1995). The embryos and larvae, reared at 19–21°C, were fixed at approximately 6 hour intervals between 3 and 5 days post-fertilization, and then at 7 days. They were fixed in 2.5 per cent (v/v) glutaraldehyde (Sigma-Aldrich Co., St Louis, MO) in filtered sea water, dehydrated in an ethanol series and cleared in benzyl benzoate/benzyl alcohol (Sigma-Aldrich Co.) 2 : 1 (v/v) and were autofluorescent.

They were observed in an Olympus FluoView FV1000 confocal laser scanning microscope incorporating an Olympus IX81 inverted microscope. For this, embryos and larvae were mounted in the clearant in a chamber made by sealing a coverslip to the underside of a hole cut in a microscope slide, which was placed on the stage of the inverted microscope. The inverted microscope gives a mirror (reflected) image of the specimen. All images, therefore, have been reflected for presentation here.

Each specimen was excited with a 488 nm argon laser and the emission collected from 500 to 600 nm. Using the FV1000 software v. 1.6.1.0, a stack of images was collected along the *z*-axis (the *Z* stack) at an optimal section thickness of 1.22 μm averaged over two frames with a 20× UplanApo objective lens NA 0.7 in a 512×512 pixel array, 8 bits/pixel. For three-dimensional imaging, the *Z* stack was rendered using maximum intensity projection, creating a three-dimensional solid image or a three-dimensional transparent image. The three-dimensional transparent image was captured in a screen print of an interactive rendering step in the FV1000 software. Images were cut from the front of the *Z* stack when creating the three-dimensional images, to view the internal structure. The *Z* stack was also viewed along the *y*-axis and along the *x*-axis, yielding sets of transverse and longitudinal sections of the larva, respectively. The resolution in the transverse and longitudinal sections was lower, 2.592 μm, when compared with a resolution of 0.386 μm in the sections from the *Z* stack itself, a property of confocal imaging (Cox 2007).

The results reported are from the observations of embryos and larvae from three fertilizations. The stage of larval development reached at similar fixation times varied between the fertilizations and within the same fertilization. The time at which hatching occurred was also variable.

(a) *Names of the five primary podia*

The primary podia are named according to the Carpenter system for echinoids as described by Hyman (1955) and as applied previously to an echinoid larva (Morris 2007). This system names the podia A–E in clockwise order in oral view, specifying that the ambulacrum opposite the madreporite is ambulacrum A. The madreporite thus lies between the ambulacra C and D. Since the madreporite forms late in the development in *P. exigua*, the stone canal connection to podium D identifies the podia here (*v.i.*).

3. RESULTS

The coordinate axes of the brachiolaria larva of *P. exigua* are set by the three brachia at the anterior end, with the central brachium lying dorsally and the two lateral brachia facing towards the ventral surface (figure 1*a*). The adhesive disc lies between the three brachia (figure 1*b*,*c*).

The coelom in the early brachiolaria larva is an epithelial-bounded cavity divisible into an anterior coelom, a left lateral coelom and a right lateral coelom (figure 1*a*). The anterior coelom projects into the central brachium and the two lateral brachia (figure 1*a*,*b*). The cavity of the coelom is continuous with the cavity of the archenteron (figure 1*a–c*). A series of transverse sections through the larva shows the transition from the brachial coelom (figure 1*d*,*e*), through the anterior coelom (figure 1*f*), to the junction with the archenteron (figure 1*g–j*), and then to the separation into the left and right lateral coeloms on either side of the archenteron (figure 1*k*). The left lateral coelom is larger than the right lateral coelom at the level of their junction with the archenteron (figure 1*i*,*j*). The pore canal, which leads from the hydropore, opens internally where the left lateral coelom and the archenteron join dorsally (figure 1*g*,*h*). Thus, in dorsal views at this early stage (figure 1*l–n*), the hydropore, lying dorsally, is close to where the left lateral coelom joins the archenteron cavity. In the left views of the larva (figure 1*o*,*p*), there is a slight constriction between the anterior portion of the left lateral coelom and its posterior portion. At a later stage, this constriction has enlarged and the anterior portion of the lateral coelom is separated from the posterior portion, which becomes the somatocoele (figure 1*q*,*r*).

(a) *Development of the five primary podia*

The five primary podia develop from the left lateral coelom and part of the anterior coelom. They appear as buds formed from the cavities and the epithelia of the two coeloms. This is shown in a series of images of an unhatched brachiolaria larva (figure 2) and a hatched brachiolaria larva (figure 3). In figure 2*a–h*, a three-dimensional transparent image is turned about the larval anterior–posterior axis from a larval dorso-left view (figure 2*a*) through a larval left view (figure 2*f*) towards a larval ventro-left view (figure 2*h*). Each of the five podia C, D, E, A and B is visible at some stage of the rotation (figure 2*a–h*). Only the three most anterior podia, B, C and D are visible in the full left view (figure 2*f*). In figure 2*i–l*, the three-dimensional transparent image is tilted about the larval dorsoventral axis towards the observer, so as to look down into the anterior coelom and the left lateral coelom. Only the podia B, C and D are visible for the first part of the tilt (figure 2*i–k*). The two most posterior podia, E and A, come into view at the end of the tilt (figure 2*l*). The hydropore and opening of the pore canal are visible through the cavity of the coelom (figure 2*k*).

A series of transverse sections (figure 2*m–w*) shows the transitions from the brachial region (figure 2*m*,*n*) through the podial region (figure 2*p–v*) to the posterior of the larva (figure 2*w*). Podia B and C are at the ventral and dorsal extremities of the podial region, respectively (figure 2*q–t*). The pore canal opens next to podia C and D (figure 2*t*).

In the series of the hatched brachiolaria larva, the three-dimensional solid image (figure 3*a*) shows the structural features of the larva, not constrained by the fertilization membrane. In figure 3*b–e*, a three-dimensional transparent image is rotated about the larval anterior–posterior axis from a larval dorso-left view (figure 3*b*) towards a larval left view (figure 3*e*). In figure 3*b*, podia C, D and E are visible and connect with the hydropore through the pore canal. In figure 3*f–h*, the three-dimensional

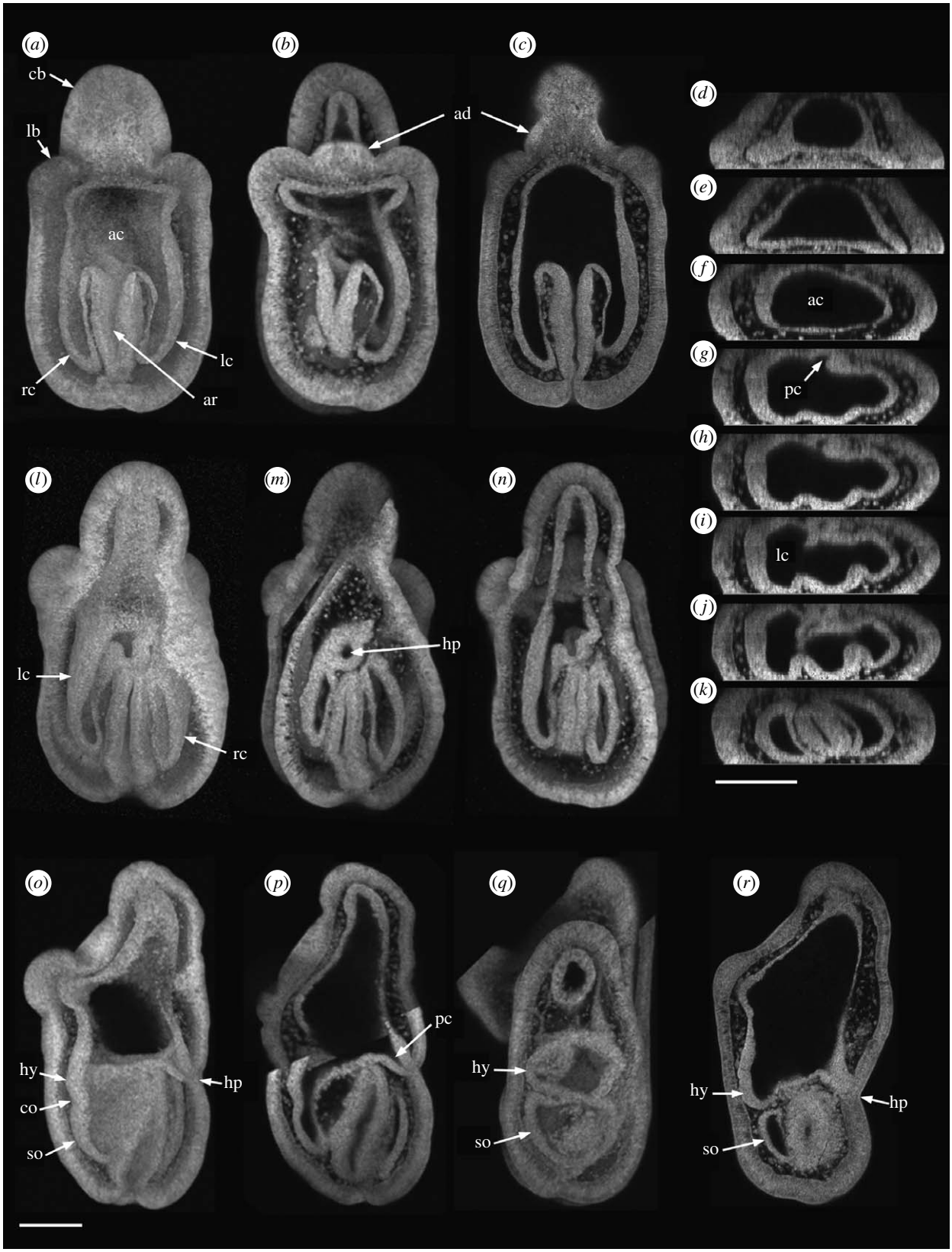

Figure 1. Confocal images of the coelom in early brachiolaria larvae constructed from the *Z* stacks of hatched larvae (described in text). (*a–c*) Ventral views of one larva: (*a*) three-dimensional solid image, (*b*) three-dimensional transparent image, (*c*) single section from the *Z* stack. (*d–k*) Single transverse sections of the larva in (*a–c*) viewed from the larval posterior with dorsal uppermost. (*l–n*) Dorsal views of one larva: (*l*) three-dimensional solid image, (*m*) three-dimensional transparent image, (*n*) three-dimensional transparent image with more images cut from the front of the *Z* stack than in (*m*). (*o*,*p*) Lateral views of one larva, dorsal right: (*o*) three-dimensional solid image, (*p*) three-dimensional transparent image. (*q*,*r*) Lateral views of two larvae, dorsal right: (*q*) three-dimensional transparent image, (*r*) single section from the *Z* stack. (*a–p*) Four-days larvae; (*q*,*r*) 4.5-days larvae. Scale bars, 100 μm. ac, anterior coelom; ad, adhesive disc; ar, archenteron; cb, central brachium; co, constriction; hp, hydropore; hy, hydrocoele; lb, lateral brachium; lc, left lateral coelom; pc, pore canal; rc, right lateral coelom; so, somatocoele.

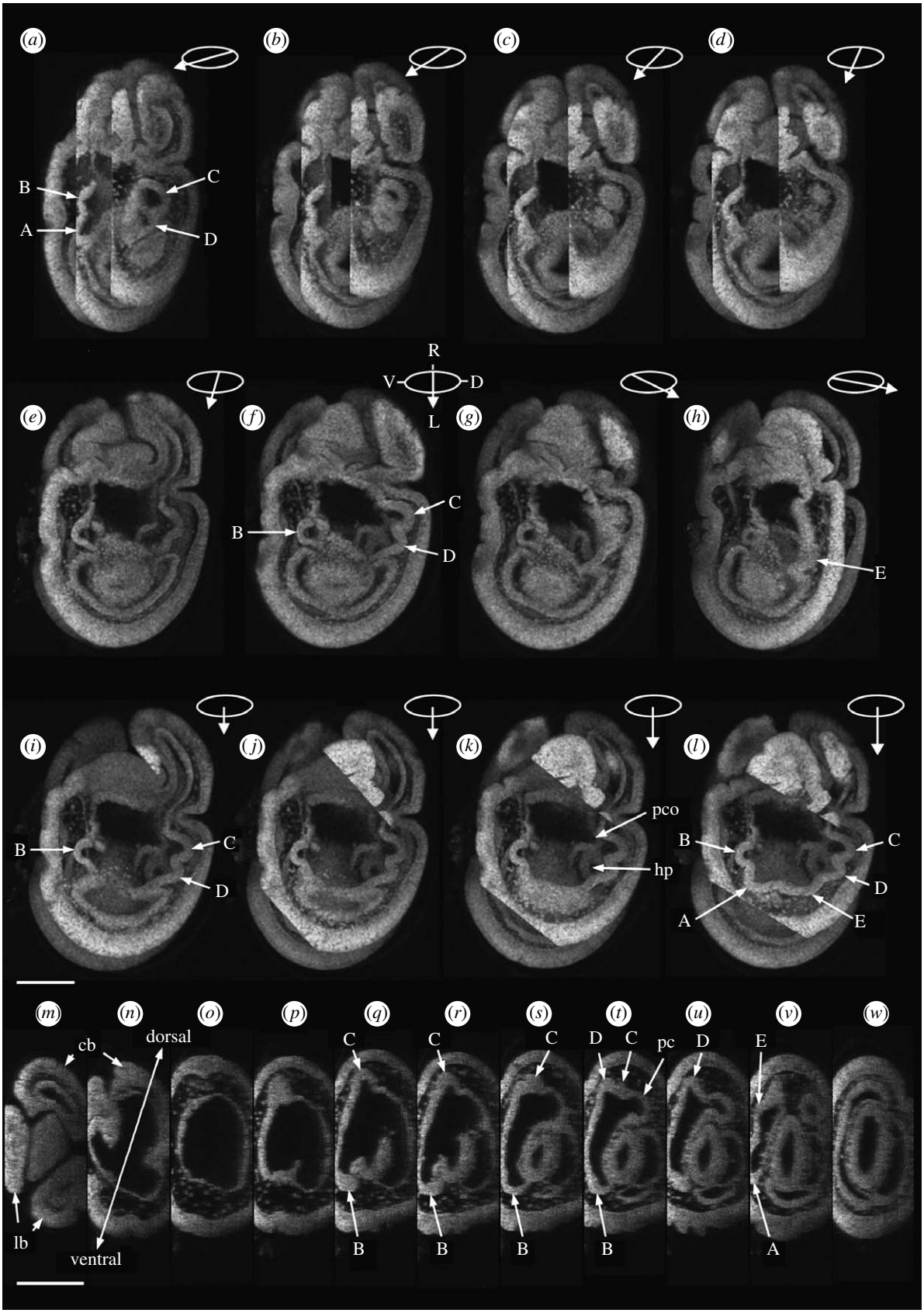

Figure 2. Confocal images of the early development of the five primary podia constructed from the *Z* stack of one unhatched brachiolaria larva (described in text). (*a–h*) The three-dimensional transparent image is rotated about the anterior–posterior axis of the larva beginning at (*a*) a dorso-left view and ending at (*h*) a ventro-left view. Ellipses with arrows show the angle of rotation: the arrow points left in each ellipse. Larval coordinates of the ellipse in *f* are D, dorsal; L, left; R, right; V, ventral. (*i–l*) The three-dimensional transparent image is tilted about the dorsoventral axis towards the observer: degree of tilt indicated by the length of the arrow in the ellipse, all are left views. (*m–w*) Single transverse sections viewed from the larval posterior, dorsal at top in each section. 3.75-days larva. Scale bars, 100 μm. A–E, podia; cb, central brachium; hp, hydropore; lb, lateral brachium; pc, pore canal; pco, opening of pore canal.

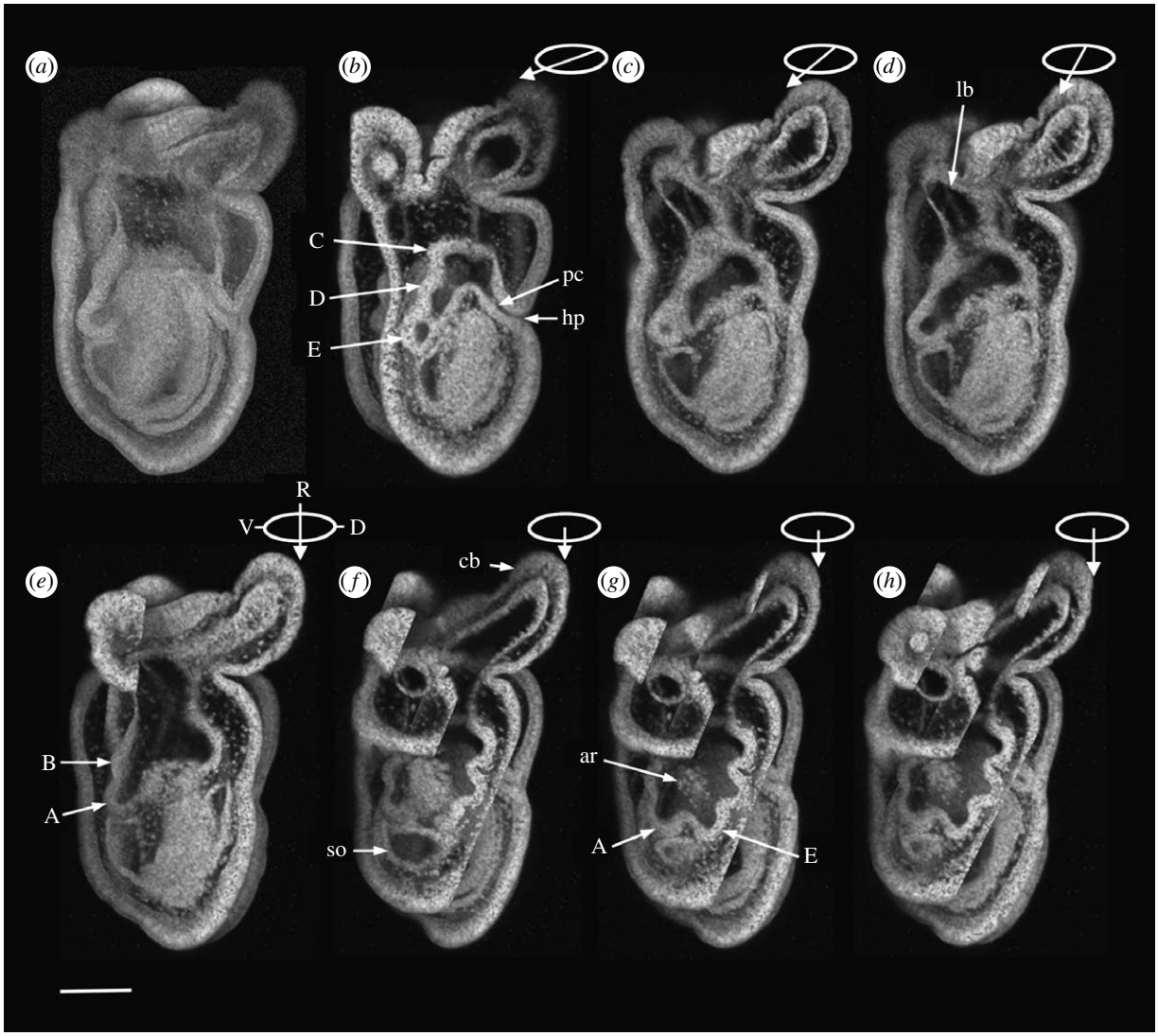

Figure 3. Confocal images of the development of the five primary podia constructed from the *Z* stack of one hatched brachiolaria larva (described in text). (*a*) Three-dimensional solid image. (*b–e*) The three-dimensional transparent image is rotated about the anterior–posterior axis of the larva from (*b*) a dorso-left view towards (*e*) a left view. Ellipses with arrows show the angle of rotation: the arrow points left in each ellipse. Larval coordinates of the ellipse in (*e*) are D, dorsal; R, right; V, ventral. (*f–h*) The three-dimensional transparent image is tilted successively towards the observer to show all five primary podia: degree of tilt indicated by the length of the arrow in the ellipse, all left views. Five-days larva. Scale bar, 100 μm. A–E, podia; ar, archenteron cells; cb, central brachium; hp, hydropore; lb, left brachium; pc, pore canal; so, somatocoele.

transparent image is tilted towards the observer, bringing the two most posterior podia, E and A, into view. Cells at the tip of the archenteron are visible centrally within the ring of podia (figure 3*g*,*h*). The anterior coelom, anterior to the archenteron, connects broadly with the coelom of the brachia.

The plane in which the podial buds lie makes an angle of approximately 40° with anterior–posterior axis of the larva (figure 3*b*,*c*). Podia C and D are dorso-left in position (figure 3*b*) while podium B is near the ventral side (figure 3*e*). The epithelium of podia C and D is continuous with the epithelium of the anterior coelom projecting into the left brachium (figure 3*d*) and with that projecting into the central brachium (figure 3*f–h*). The other two podia, E and A, are more posterior in position than podia C, D and B (figure 3*g*,*h*).

Thus it is that the five primary podia form from the coelomic epithelium and coelomic cavity on the left side of the larva that is above and below the level of the inner termination of the archenteron.

(b) *Later development*

In a late brachiolaria larva, a constriction partly separates a posterior region housing the adult rudiment from the brachial region, which lies anteriorly (figure 4*a*,*b*). The five primary podia are shown in a three-dimensional transparent image in oral view (figure 4*a*). In a single section at an aboral level (figure 4*b*), podium B connects with the left anterior coelom and the pore canal connects with the right anterior coelom. A selected series of transverse sections between the podia and the brachia (figure 4*c–h*) shows the relationships between the podial coeloms, the left and right anterior coeloms, the common anterior coelom and the brachial coelom. The podia A, E and D in figure 4*c* are all joined in figure 4*d*. In figure 4*e*, podium B connects with the left anterior coelom. In figure 4*f*, podium C connects with the left anterior coelom. The left anterior coelom is separated from the right anterior coelom by the tip of the archenteron in figure 4*f*. In figure 4*g*, the left anterior coelom joins the right anterior coelom (figure 4*f*) over the archenteron

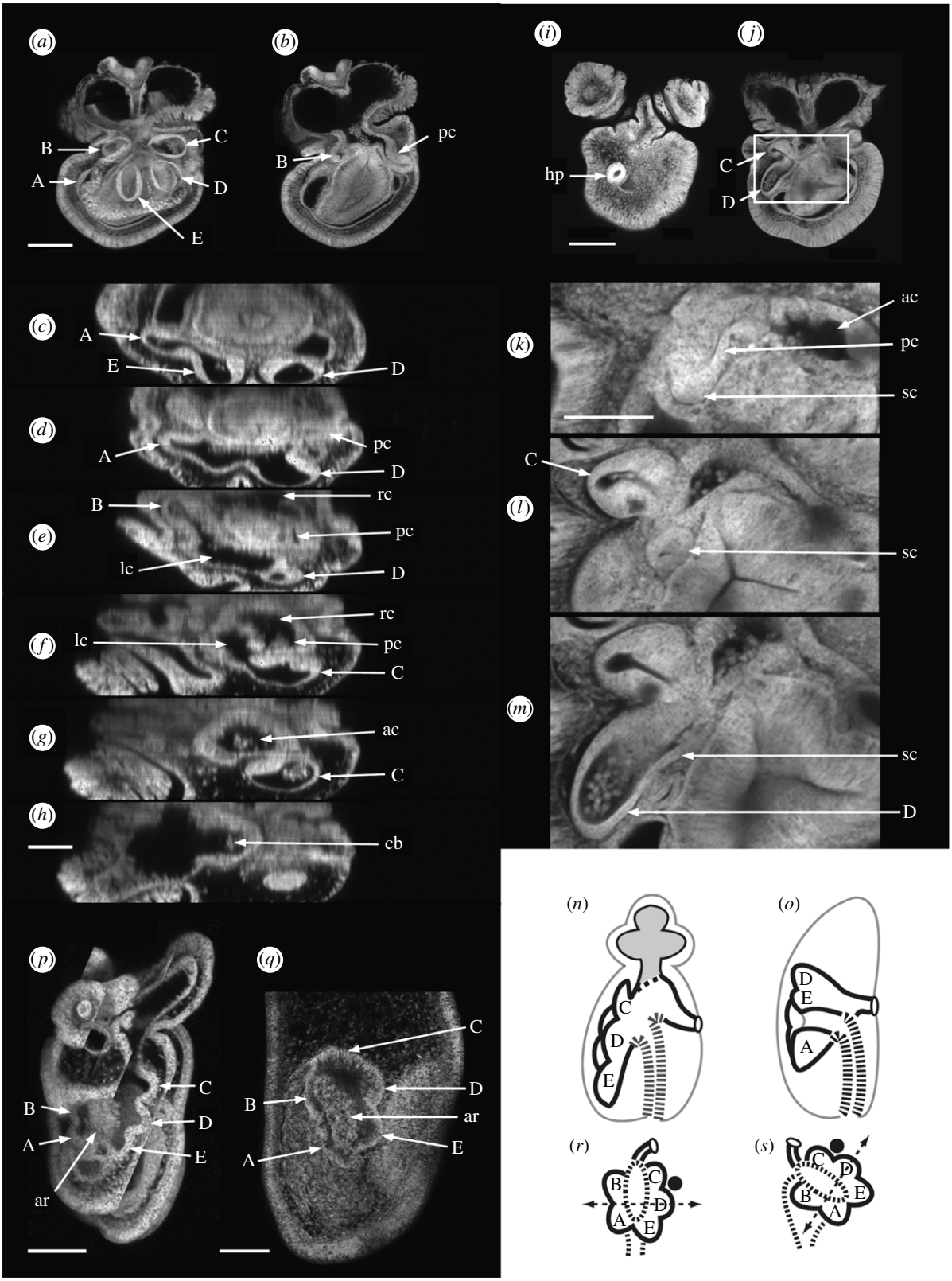

Figure 4. (*a–h*) Confocal images of the later development of the coeloms in a late brachiolaria larva constructed from the *Z* stack of one larva (described in text). (*a*) Three-dimensional transparent image, larval left view. (*b*) Single section deeper in the *Z* stack, larval left view. (*c–h*) Selected transverse sections from the podial regions to the brachia viewed from the larval anterior, dorsal at right in each section. (*i–m*) The pore canal and the stone canal in a late brachiolaria larva (described in text). (*i,j*) Single sections from the *Z* stack, dorsal view. (*k–m*) Enlargements of images selected from the *Z* stack within the boxed region in *j*. Seven-days larvae. (*p,q*) Homology of the primary podia in the asteroid *P. exigua* (*p*) and the echinoid *Holopneustes purpurescens* (*q*) (described in text). Scale bars, 100 μm, except in (*k*), 50 μm. A–E, label the podia; ac, anterior coelom; ar, archenteron; cb, central brachial coelom; hp, hydropore; lc, left anterior coelom; pc, pore canal; rc, right anterior coelom; sc, stone canal. (*n,o*) Common structures of (*n*) the asteroid and (*o*) the echinoid body plans (described in text), sagittal views, oral left. (*r,s*) Interpretive diagram of the homology between (*r*) the asteroid and (*s*) the echinoid primary podia (described in text). Black spot, madreporite; dashed line with arrows, the anterior–posterior axis of the primary podia (Morris 2007); shaded coelom, brachial coelom; thick dashed line, archenteron wall.

tip and this common anterior coelom joins the brachial coelom (figure 4*h*).

On the right side of the series, the pore canal opens into the right anterior coelom (figure 4*d–f*) which, via the anterior coelom, is in communication with the podial coeloms on the left side, via the left anterior coelom, as in figure 4*b*.

(c) *Criterion for naming the podia*

In early brachiolaria larvae (figures 2 and 3), the pore canal connects with the podia indirectly through the anterior coelom. In late brachiolaria larvae, another canal is seen, the stone canal, and it connects podium D to the pore canal close to where the pore canal joins the anterior coelom. The stone canal connection to podium D is the criterion for naming the podia.

The morphology is shown in figure 4*i–m*. The pore canal opens externally on the aboral surface of the brachiolaria larva at the hydropore (figure 4*i*). The internal path of the pore canal between the section in figure 4*i* and that in figure 4*j* is shown in enlarged views (figure 4*k–m*) selected from the region boxed in figure 4*j*. In figure 4*k*, the pore canal connects with the anterior coelom while the stone canal appears as a bud on the pore canal, directed posteriorly. The stone canal is a separate profile in figure 4*l*, and in figure 4*m* it joins podium D.

(d) *Metamorphosis*

During metamorphosis, the brachial coelom of the larva is withdrawn into the adult coeloms. In our images (not shown), the connection between the brachial coelom and the anterior coelom is always separated from the podial coeloms, suggesting that the brachial coelom is withdrawn into the anterior coelom, rather than into the hydrocoele. Connected to the anterior coelom is the pore canal, and a branch from the pore canal, the stone canal, goes to podium D. Thus, at the completion of metamorphosis, the anterior coelom has connections to the exterior via the pore canal and to the hydrocoele via the stone canal. The anterior coelom also contains the tip of the archenteron that has been brought close to the constricted bases of the podia at the centre of the hydrocoele (figure 4*m*).

4. DISCUSSION

The description we give for *P. exigua* of the podial and anterior larval coeloms and the conversion to the juvenile form is similar to the descriptions in the early literature of these structures and processes in *Asterias rubens* (Gemmill 1914) and *Asterina gibbosa* (MacBride 1896). In these species, the primary podia appear as buds at the edges of a crescentic hydrocoele formed from the left coelom. The hydrocoele is open to the anterior coelom and, at metamorphosis, the brachial coelom is withdrawn into the adult coeloms. The path of the withdrawal differs between asteroid species: in *A. rubens* (Gemmill 1914) and *A. gibbosa* (MacBride 1896), the hydrocoele is described as encircling the connection with the brachial coelom but in *Cribrella* (=*Henricia*) the withdrawal is to one side of a closed hydrocoele (Masterman 1902), as it is in *P. exigua*. The end result of the withdrawal in these species, which is of an anterior coelom with connections to the exterior and to the hydrocoele, is, however, the same. The anterior coelom is also where, in *A. rubens*, the retained portion of the larval gut is brought towards the centre of the hydrocoele ring, where the mouth later forms (Gemmill 1914, p. 263).

The primary podia in *A. rubens* (Gemmill 1914) are numbered I–V in a clockwise series around the crescent of the hydrocoele in oral view, with podium I in a larval anterior-dorsal position and podium V in a larval anterior-ventral position. Using the Carpenter system (Hyman 1955; Morris 2007), we can name these podia C, D, E, A and B starting at podium I, by using the names of the podia in *P. exigua*. Our criterion for naming the podia in *P. exigua* is the connection of the stone canal to podium D, which is in reasonable agreement with Gemmill (1914, p. 257), who described the inner opening of the stone canal in *A. rubens* to be between podia I and II and in *Solaster endeca* to be opposite podium II.

We used the connection of the stone canal to podium D as the criterion for naming the podia in *P. exigua* since the madreporite, which is the criterion used in echinoids, had not yet formed. The madreporite is expected to form between arm rudiments I and II, as it does in *A. rubens* (Gemmill 1914; Gondolf 2000), that is, between arm rudiments C and D in *P. exigua*: if it does, it would support the use of the stone canal connection to podium D for naming the podia. We suggest that the stone canal with a precise connection to podium D is a reliable way of naming the podia between the echinoderm classes, among the other criteria that have been used (Hotchkiss 1998). In the echinoid *Holopneustes purpurescens* (Morris 1995), the stone canal connects to podium D (V. B. Morris 2008, unpublished data), where podium D is identified using the madreporite (Morris & Byrne 2005).

(a) *Homology*

The similarities in development noted between the asteroid species from different orders bring to attention the core structures of the asteroid radiate body plan. These are the podial coeloms, which constitute the hydrocoele, and their connection to the exterior through the pore canal and hydropore. Homology with the echinoid class is therefore to be found between these core structures, which are illustrated in figure 4*n*,*o*.

The homology between the asteroid and the echinoid primary podia is shown in figure 4*p*,*q*. In the asteroid *P. exigua* (figure 4*p*), three podia, C, D and E, lie to one side of the archenteron and two podia, A and B, lie to the opposite side. In the echinoid *H. purpurescens* (figure 4*q*), a similar relationship is seen, with podia C, D and E on one side of the archenteron and podia A and B on the other; but in this species, the close relationship between the coeloms that form the podia and the archenteron wall shows the region of the inner archenteron wall from which the podia develop. In *H. purpurescens*, podia C, D and E form from the dorsal wall of the archenteron and podia A and B form from the ventral wall of the archenteron (Morris 2007).

The relationship of the primary podia to specific regions of the inner archenteron wall seen directly in *H. purpurescens* and indirectly in *P. exigua* demonstrates a regional specialization of the inner archenteron wall with respect to coelom formation and in turn to the structures that develop from the coeloms. Such regional specialization might well determine body plan architecture dependent on how the inner archenteron is positioned

with respect to the embryonic body axes. In an interpretive diagram (figure 4*r*,*s*), we show the podial–archenteron relationship in an asteroid and an echinoid. With the relationship of the podia to the inner archenteron wall kept unchanged, a difference in the positions of the podia between the asteroid and the echinoid is explained by a rotation of the transverse axis of the inner archenteron in the echinoid that is anticlockwise with respect to the axis in the asteroid.

Extending the idea of a conserved regional specialization of the inner archenteron to other deuterostome phyla gives a source for the homology between the deuterostome phyla, leading to inferences of homologous structures. For example, the coelomic regions of the C, D, E podia and the pore canal and hydropore in asteroids and echinoids (figure 4*r*,*s*) could be considered homologous with the coelomic regions of the proboscis coelom and the pore canal in hemichordates, accepting an adjustment of the position and orientation of the inner archenteron wall of the hemichordate relative to the hemichordate embryonic body axes. Extending the procedure to chordates, the coelomic region of the C, D, E podia could be considered homologous with the chordate notochord, given a repositioning of the inner archenteron with respect to the chordate embryonic body axes. The required repositioning is a complete foreshortening of the archenteron such that the inner archenteron wall lies close to the blastopore from which it originates, as in the primitive streak of land vertebrates. The C, D, E podial forming region would then lie in the position of Henson's node at the dorsal end of the primitive streak and the notochord would be expected to form from this region of the archenteron, which it does.

Such a scenario for chordates offers an explanation of the differences in gene expression on the dorsal and ventral sides of hemichordates and vertebrates (Lowe *et al.* 2006), which are currently explained by the dorsoventral inversion hypothesis for chordates (Arendt & Nübler-Jung 1994; De Robertis & Sasai 1996). The gene *chordin*, for example, in a hemichordate, is expressed on the ventral side where the mouth is, whereas it is expressed on the dorsal side in a vertebrate (Lowe *et al.* 2006). Our scenario does not require that chordates inverted their dorsoventral body axis.

Thus, evidence of structural commonalities in the body plans of the echinoderm classes progresses the search for the structural homology of the deuterostome phyla.

We thank Paula Cisternas for donating cultures of *P. exigua*. We acknowledge the facilities and the scientific and technical assistance from the staff of the Australian Microscopy & Microanalysis Facility at the Electron Microscope Unit, The University of Sydney.

REFERENCES

Arendt, D. & Nübler-Jung, K. 1994 Inversion of dorsoventral axis? *Nature* **371**, 26. (doi:10.1038/371026a0)

Byrne, M. 1995 Changes in larval morphology in the evolution of benthic development by *Patiriella exigua* (Asteroidea: Asterinidae), a comparison with the larvae of *Patiriella* species with planktonic development. *Biol. Bull.* **188**, 293–305. (doi:10.2307/1542306)

Cox, G. 2007 *Optical imaging techniques in cell biology*. Boca Raton, FL: CRC Press, Taylor & Francis.

David, B. & Mooi, R. 1996 Embryology supports a new theory of skeletal homologies for the phylum Echinodermata. *CR Acad. Paris* **319**, 577–584.

De Robertis, E. M. & Sasai, Y. 1996 A common plan for dorsoventral patterning in Bilateria. *Nature* **380**, 37–40. (doi:10.1038/380037a0)

Gemmill, J. F. 1914 The development and certain points in the adult structure of the starfish *Asterias rubens* L. *Phil. Trans. R. Soc. B* **205**, 213–294. (doi:10.1098/rstb.1914.0016)

Gondolf, A. L. 2000 Light and scanning electron microscopic observations on the developmental biology of the common starfish *Asterias rubens* Linné (Echinodermata: Asteroidea). *Ophelia* **52**, 153–170.

Hotchkiss, F. H. C. 1998 A 'rays-as-appendages' model for the origin of pentamerism in echinoderms. *Paleobiology* **24**, 200–214.

Hyman, L. H. 1955 *The invertebrates: Echinodermata IV*. New York, NY: McGraw-Hill.

Lowe, C. J. *et al.* 2006 Dorsoventral patterning in hemichordates: insights into early chordate evolution. *PLoS Biol.* **4**, 1603–1619. (doi:10.1371/journal.pbio.0040291)

MacBride, E. W. 1896 The development of *Asterina gibbosa*. *Q. J. Microsc. Sci.* **38**, 339–411.

Masterman, A. T. 1902 The early development of *Cribrella oculata* (Forbes), with remarks on echinoderm development. *Trans. R. Soc. Edin.* **40**, 373–417.

McEdward, L. R. & Janies, D. A. 1993 Life cycle evolution in asteroids: what is a larva? *Biol. Bull.* **184**, 255–268. (doi:10.2307/1542444)

Morris, V. B. 1995 Apluteal development of the sea urchin *Holopneustes purpurescens* Agassiz (Echinodermata: Echinoidea: Euechinoidea). *Zool. J. Linn. Soc.* **114**, 349–364. (doi:10.1111/j.1096-3642.1995.tb00120.x)

Morris, V. B. 2007 Origins of radial symmetry identified in an echinoderm during adult development and the inferred axes of ancestral bilateral symmetry. *Proc. R. Soc. B* **274**, 1511–1516. (doi:10.1098/rspb.2007.0312)

Morris, V. B. & Byrne, M. 2005 Involvement of two Hox genes and *Otx* in echinoderm body-plan morphogenesis in the sea urchin *Holopneustes purpurescens*. *J. Exp. Zool. B* (*Mol. Dev. Evol.*) **304**, 456–467. (doi:10.1002/jez.b.21065)

Peterson, K. J., Arenas-Mena, C. & Davidson, E. H. 2000 The A/P axis in echinoderm ontogeny and evolution: evidence from fossils and molecules. *Evol. Dev.* **2**, 93–101. (doi:10.1046/j.1525-142x.2000.00042.x)

Swalla, B. J. & Smith, A. B. 2008 Deciphering deuterostome phylogeny: molecular, morphological and palaeontological perspectives. *Phil. Trans. R. Soc. B* **363**, 1557–1568. (doi:10.1098/rstb.2007.2246)

Ubaghs, G. 1967 General characters of Echinodermata. In *Treatise on invertebrate paleontology. Part S Echinodermata 1*, (ed. R. C. Moore) pp. S3–S60. Lawrence, KS: The University of Kansas and the Geological Society of America, Inc.